Macromolecules

Article

pubs.acs.org/Macromolecules

Template-Directed Synthesis of Structurally Defined Branched Polymers

Amanda B. Marciel,[†] Danielle J. Mai,[‡] and Charles M. Schroeder*[,†,‡,§,∥]

[†]Center for Biophysics and Quantitative Biology, [‡]Department of Chemical and Biomolecular Engineering, [§]Department of Chemistry, and [∥]Department of Materials Science and Engineering, University of Illinois at Urbana−Champaign, Urbana, Illinois 61801, United States

Supporting Information

ABSTRACT: A grand challenge in materials chemistry is the synthesis of macromolecules and polymers with precise shapes and architectures. In this work, we describe a hybrid synthetic strategy to produce structurally defined branched polymer architectures based on chemically modified DNA. Overall, this approach enables precise control over branch placement, grafting density, and chemical identity of side branches. We utilize a two-step scheme based on polymerase chain reaction (PCR) for site-specific incorporation of non-natural nucleotides along the main polymer backbone, followed by copper-free "click" chemistry for grafting side branches at specific locations. In this way, linear DNA backbones are first synthesized via PCR by utilizing the promiscuity of a high yield thermophilic DNA polymerase to incorporate nucleotides containing bioorthogonal dibenzocyclooctyne (DBCO) functional groups at precise locations along one strand of the DNA backbone. Following PCR, copper-free "click" chemistry is used to attach synthetic polymer branches or oligonucleotide branches to the DNA backbone, thereby allowing for the synthesis of a variety of precise polymer architectures, including three-arm stars, H-polymers, and graft block copolymers. Branched polymer architectures are characterized using polyacrylamide gel electrophoresis, denaturing high performance liquid chromatography (HPLC), and matrix-assisted laser desorption/ionization (MALDI) mass spectrometry. In a proof-of-principle demonstration, we synthesize miktoarm stars with AB_2 structures via attachment of mPEG-azide branches (1 and 10 kDa) at precise locations along a DNA backbone, thereby expanding the chemical functionality of structurally defined DNA topologies.

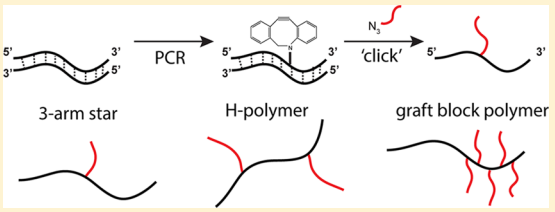

INTRODUCTION

The development of advanced materials critically relies on the synthesis of structurally defined and sequence-defined polymers. Precise control over the spatial position of chemical groups along a polymer chain backbone holds the key to generating polymers that can self-assemble into hierarchical supramolecular structures or perform complex functions. To this end, extensive efforts have been focused on the development of synthetic methods that can provide simultaneous control over polymer composition, topology, and chemical functionality with a high degree of polymer chain uniformity.[1−7] Several synthetic strategies have been developed in recent years with increased control over polymer chain properties, including controlled living radical polymerization based on stable free radicals, degenerative transfer, and atom transfer radical polymerizations (ATRP).[2,9,10] ATRP has been used to produce architecturally complex polymers including star, comb/brush, and hyperbranched topologies with controlled molecular weights and narrow molecular weight distributions.[11−18] However, ultimate control over macromolecular structure and molecular weight distribution has yet to be achieved using purely synthetic methods.

To overcome these challenges, techniques from molecular biology and solid-phase synthesis have been used to produce monodisperse, sequence-defined peptide-based and nucleic acid-based polymers.[1−10] In this way, the natural self-assembly behavior of double-stranded DNA has been exploited to generate functional materials due to predictable secondary structure formation.[19] In particular, biomimetic or biohybrid polymers based on DNA are able to self-assemble by directed hydrogen bond formation via oligonucleotide hybridization. As a consequence, several DNA nanostructures are composed of rationally designed, chemically synthesized oligodeoxynucleotides.[19−22] DNA nanostructures have also been constructed using monodisperse samples of short- and long-chain DNA sequences, which are routinely prepared via polymerase chain reaction (PCR) or extracted from genomic sources (e.g., M13 phage DNA). Enzymatic template-directed synthesis enables rapid production of monodisperse and sequence-defined DNA-based polymers. Despite these key advantages, however, natural DNA lacks the broad chemical diversity generally provided by synthetic polymers that are routinely employed as functional materials.

In order to incorporate chemical functionality into nucleic acid polymers, DNA can be readily modified using a variety of approaches. DNA block copolymers (DBCs) have been

Received: February 1, 2015
Revised: February 13, 2015
Published: February 25, 2015

DOI: 10.1021/acs.macromol.5b00219
Macromolecules 2015, 48, 1296−1303

synthesized via covalent attachment of oligonucleotides to synthetic organic polymers, thereby allowing for self-assembly and tuning of behavior by controlling one or both blocks.[23] Recently, amphiphilic DBCs exhibiting micelle-like assembly behavior have been synthesized, and these structures have proven useful for applications in biotechnology and nanomedicine.[24−26] The first generation of DBCs was based on a linear chain architecture, whereas many industrially relevant synthetic organic polymers are known to have exceedingly complex topologies. Therefore, an alternative class of DBCs with branched architectures was subsequently synthesized consisting of synthetic polymer backbones with randomly grafted DNA side chains. This strategy has been used to synthesize comb polymer architectures based on poly(acrylic acid) backbones for single-nucleotide polymorphism detection,[27] ROMP-derived backbones for DNA detection,[28,29] biodegradable polypeptide backbones for hydrogel formation,[30] and poly(peptide) nucleic acid amphiphiles for nanoparticle formation.[31] These synthetic strategies, however, do not allow for precise control over branch placement, grafting density, and chain uniformity.

In a related approach, a handful of studies have focused on synthesizing DNA backbones with grafted polymer side chains. Here, DNA intercalators can be used to cross-link double-stranded DNA upon UV irradiation, followed by covalent attachment of synthetic polymers.[32−34] This strategy produces monodisperse backbone molecular weights via plasmid DNA; however, it similarly lacks precise control over branch density and placement. A subsequent investigation used the ability of DNA polymerase to incorporate non-natural nucleotide triphosphates containing large polymer modifications in a template-dependent manner.[35] However, nucleotides containing substantial chemical modifications exhibited exceedingly poor fidelity by a natural DNA polymerase, which inhibits manipulation of branch length and chemical identity. From this perspective, there remains a strong need for the development of new techniques and methods allowing for precise topological control of polymers.

In this work, we demonstrate a versatile synthesis method to produce monodisperse and architecturally precise branched polymers based on single-stranded DNA (ssDNA) backbones. In particular, we use a hybrid enzymatic graft-onto synthesis method, thereby allowing for precise control over side branch placement along ssDNA backbones. First, we utilize the natural ability of *Pwo* superyield DNA polymerase to enzymatically incorporate chemically modified DBCO-dUTP monomers in a template-directed fashion. Next, we employ copper-free "click" chemistry to directly graft natural oligonucleotides or synthetic polymer side branches onto ssDNA backbones. In this way, we systematically produce a variety of branched ssDNA architectures including three-arm stars, H-polymers, and graft block copolymers with uniform composition, topology, and chemical identity. From a broad perspective, this synthetic strategy could provide a useful method for the facile production of polymers with model topologies for structure−property relationship studies.

EXPERIMENTAL SECTION

Backbone Synthesis. Polymerase chain reaction (PCR) is used to generate monodisperse linear DNA with high degrees of spatial control over functional groups (i.e., grafting sites) along the polymer backbone. In this way, we use PCR as a template-directed synthesis method to produce chemically modified DNA that serves as the main-chain backbone for branched polymers. Template DNA sequences are designed by positioning dATP nucleotides along a double-stranded DNA backbone such that dATP is present only in the complementary strand of the desired product single-stranded DNA. DNA templates (Integrated DNA Technologies, 1 ng) are enzymatically amplified in the presence of reverse and forward DNA oligonucleotide primers (Integrated DNA Technologies, 200 nM), dATP, dGTP, dCTP (New England BioLabs, 200 μM), DBCO-dUTP nucleotide (Jena Biosciences, 200 μM), *Pwo* superyield buffer (Roche, 1.5 mM $MgSO_4$), and *Pwo* superyield polymerase (Roche, 1 unit) using a Bio-Rad C1000 Touch Thermal cycler via the following protocol: 94 °C for 30 s, [94 °C for 15 s, 57 °C for 30 s, 72 °C for 20 s] repeated 25×, 72 °C for 4 min. In this way, we are able to produce a double-stranded DNA product such that one strand contains the chemically modified DBCO-dUTP nucleotide with precise control over the location. PCR amplicons are purified using an Amicon spin column (10 kDa MWCO) at 7500*g* for 50 min in a Thermo Scientific Sorvall Legend RT+ centrifuge. Final concentrations were determined via absorption at 254 nm using a Thermo Scientific NanoDrop 1000 spectrophotometer.

Graft-Onto Branching Reaction. Strain-promoted [3 + 2] azide−alkyne cycloaddition (SPAAC) was used to produce branched DNA polymers. DBCO-modified amplicons (concentration determined via absorption at 254 nm) are reacted with 10-fold molar excess azide-modified branch molecules for 12 h at 70 °C while shaking at 300 rpm using an Eppendorf thermomixer in standard reaction buffer (300 mM NaCl, 10 mM Tris/Tris HCl pH 7.5, 1 mM EDTA). In this work, side branches are varied to include DNA oligonucleotides and synthetic polymers of different molecular weight.

Polyacrylamide Gel Electrophoresis. Gel electrophoresis is used to characterize linear polymer precursors and branched polymer architectures. Polyacrylamide gels (12%) are first equilibrated in 1× TBE buffer (Bio-Rad) for 20 min at 60 V via a Bio-Rad PowerPac Basic. Branched polymer samples (2 μL) were prestained with SYBR Gold nucleic acid gel stain (1X, Life Technologies) and run at 60 V until samples entered the gel matrix, followed by a standard run at 120 V for 60 min. Polyacrylamide gels are imaged using an appropriate excitation/emission filter (e.g., ethidium bromide filter) using a Foto/Analyst FX (FotoDyne Incorporated). Dual colored polyacrylamide gels are imaged with SYBR Gold and Cy5 filters using a Bio-Rad Gel Doc. In all cases, branched polymer samples are run on gels containing a low molecular weight DNA ladder as a size standard (New England BioLabs).

Denaturing High-Performance Liquid Chromatography. Denaturing high-performance liquid chromatography (DHPLC) was used to isolate final polymer products based on ssDNA branched polymers (Agilent Technologies 1100 series LC). First, double-stranded DNA branched polymers are heated to 70 °C for 2.5 min and injected onto poly(styrene−divinylbenzene) particle reversed-phase columns (Agilent Technologies, PLRP-S) heated to 70 °C. In this way, the template molecule and branched polymer architecture are denatured during column purification, thereby enabling facile separation and isolation via differences in size and hydrophobicity. The mobile phase was 0.1 M triethylammonium acetate (TEAA) buffer at pH 7, and products were eluted using a linear acetonitrile gradient (0−100% over 100 min) in 0.1 M TEAA using a flow rate of 0.3 mL/min. Samples are monitored in real time via UV absorbance at 254 nm, and isolated products are concentrated via a miVac Duo Concentrator (Genevac) and resuspended in the appropriate buffer for chemical characterization.

Matrix-Assisted Laser Desorption/Ionization (MALDI) Mass Spectrometry. Samples isolated from DHPLC were resuspended in 12 μL of distilled, deionized water (ddH_2O). In order to rapidly assay the samples before MALDI, a small amount of sample is analyzed using polyacrylamide gel electrophoresis to assess sample integrity and purity. Polymer molecular weights are then determined (1 μL of sample with 1 μL of 3-hydroxypicolinic acid (3HPA)) using matrix-assisted laser desorption/ionization mass spectrometry (UltrafleXtreme MALDI/TOF-TOF, Bruker Daltonics).

DOI: 10.1021/acs.macromol.5b00219
Macromolecules 2015, 48, 1296−1303

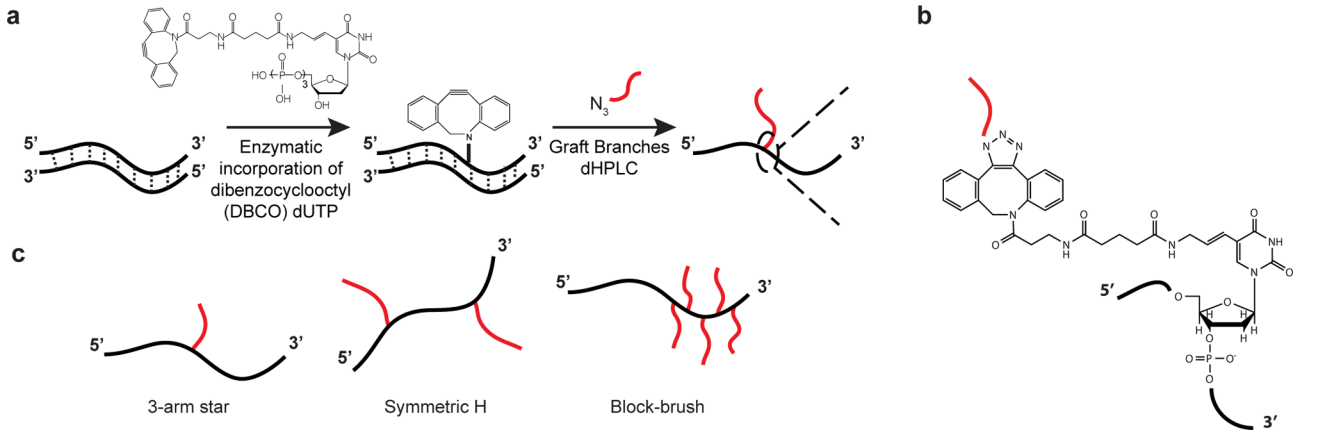

Figure 1. Synthesizing structurally defined polymers based on DNA. (a) Schematic of hybrid two-step synthesis method for polymers with precise topologies. Template-directed synthesis is used to generate dibenzocyclooctyne (DBCO)-modified DNA, thereby enabling precise placement of bioorthogonal branch sites along a polymer backbone. In a second step, azide-terminal polymers are attached to the polymer backbone at specific sites via copper-free "click" chemistry using a graft-onto approach. (b) Chemical structure of linkage between DBCO-dUTP and the azide-terminated polymer branch (red). (c) Topologies of polymers consisting of 1, 2, or 5 branch sites used to synthesize three-arm stars, H-polymers, and graft block polymers, respectively.

RESULTS AND DISCUSSION

In this work, we demonstrate a method to synthesize structurally defined polymers based on chemically modified DNA. Using this approach, we generate branched polymers consisting of ssDNA backbones containing chemically grafted ssDNA branches or synthetic polymer branches at precise locations (Figure 1). The synthetic method is a two-step process consisting of enzymatic template-directed synthesis via PCR, followed by a graft-onto reaction using copper-free "click" chemistry. First, PCR is used to enzymatically amplify custom oligonucleotide DNA templates, thereby enabling precise placement of bioorthogonal reactive sites that serve as branch points along a polymer backbone (Figure 1a). Because of the template-directed nature of PCR, total replacement of natural dTTP nucleotides with modified 5-dibenzylcyclooctyne dUTP (DBCO-dUTP) nucleotides allows for precise and exact placement of reactive sites along one strand of a double-stranded DNA backbone (Figure 1a,b). Prior work has shown that several native and engineered DNA polymerases (e.g., *Pwo*, *Pfu*, *Vent* (*exo-*), *Deep Vent* (*exo-*), *KOD Dash*) directly incorporate non-natural nucleotides with modifications at the C5 position of pyrimidine and the C7 and C8 positions of purine.[36,37] In this study, we use the high fidelity *Pwo* DNA polymerase to incorporate chemically modified DBCO-dUTP nucleotides, which contain a DBCO moiety linked to the C5 position of the pyrimidine nucleobase.

Following PCR, polyacrylamide gel electrophoresis is used to qualitatively assay for the desired reaction product, which is indicated by the appearance of a single product band at the desired molecular weight (Figure S1). Negative controls show negligible evidence of product formation (e.g., absence of dTTP or non-natural DBCO-dUTP nucleotide yields no product), which is expected based on the high fidelity of *Pwo* DNA polymerase. In this way, we are able to generate precursor DNA templates for a variety of topologies including 3-arm stars (Figure S1), H-polymers (Figure S8), and block graft copolymers (Figure S17). To quantitatively assay for incorporation of non-natural DBCO-dUTP nucleotides, we utilized a combination of reversed-phase denaturing high-performance liquid chromatography (DHPLC) and MALDI mass spectrometry. DHPLC allows for resolution of ssDNA polymers (<100 nucleotides) of identical length and differing base composition.[38] Using this approach, we are able to isolate the desired product ssDNA strands containing non-natural DBCO from the complementary natural template strands for 3-arm star templates (Figure S2), H-polymer templates (Figure S9), and block graft copolymer templates (Figure S18). Finally, in all cases, the identity of polymer templates is unambiguously determined via MALDI mass spectrometry (Figures S3, S10, and S19).

Following chemical characterization of linear polymer precursors, strain-promoted [3 + 2] azide−alkyne cycloaddition (SPAAC) was employed to covalently attach azide-terminal side branch polymers to DBCO-dsDNA products, thereby producing branched polymer architectures (Figure 1a,b). SPAAC reactions are ideal for DNA modification due to bioorthogonality as well as high solvent and functional group tolerance.[39−41] Using this approach, we designed oligonucleotide sequences with 1, 2, or 5 bioorthogonal branch sites, thus facilitating formation of three-arm star, H-polymer, and graft block copolymer architectures, respectively (Figure 1c).

Three-arm star polymers are the simplest branched architectures consisting of three linear polymer chains attached to a single central core.[3,42] Three-arm star topologies have gained interest because branch number, branch length, and chemical identity can be independently modified to manipulate bulk morphologies.[3,42] We began by synthesizing homopolymeric three-arm star architectures with 25-mer oligonucleotide symmetric arms via attachment of an azide-terminal 25-mer oligonucleotide to the central monomer (corresponding to base 26) of a 51-base-pair DBCO-dsDNA product. Following chemical synthesis and purification, three-arm star polymers were analyzed via polyacrylamide gel electrophoresis and exhibited reduced electrophoretic mobility through the gel matrix as compared to linear DNA or negative control samples consisting of reactions using linear dsDNA without DBCO modifications (Figure 2a). These results are consistent with previous studies that have shown substantially reduced electrophoretic mobility of branched architectures produced by DNA hybridization, that is, branched DNA-based polymers formed by noncovalent base pairing (hydrogen bonding) rather than covalent bond formation.[43−46]

DOI: 10.1021/acs.macromol.5b00219
Macromolecules 2015, 48, 1296−1303

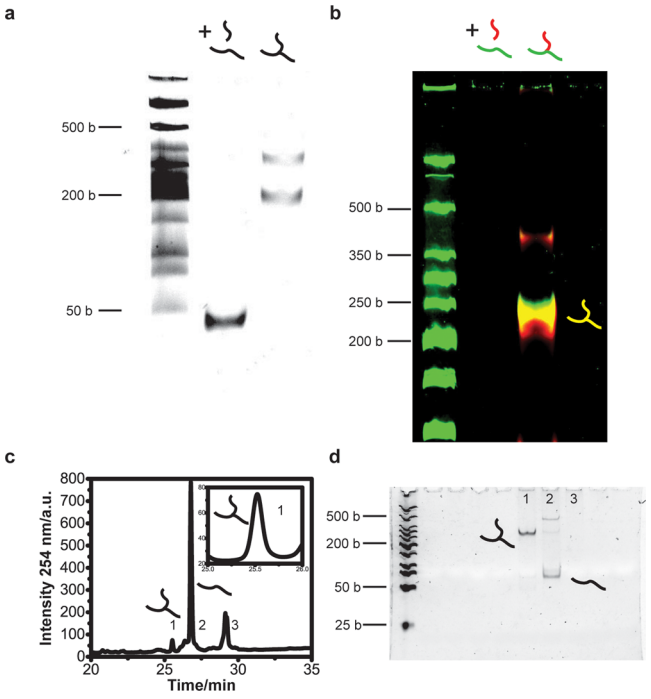

Figure 2. Synthesis and purification of structurally defined three-arm star polymers. (a) Polyacrylamide gel electrophoresis of three-arm stars consisting of 25-mer oligonucleotide arms. Lane 1: negative control consisting of natural DNA backbones reacted with an azide-terminated 25-mer oligonucleotide. Lane 2: three-arm stars are synthesized by grafting azide-terminated 25-mer oligonucleotides to the central monomer of a 51-base-pair DNA. Formation of the branched polymer topology is indicated by reduced electrophoretic mobility, a complex banding pattern, and absence of the DBCO-dsDNA linear backbone. (b) Two-color fluorescence polyacrylamide gel electrophoresis of three-arm stars with Cy5-modified azide-terminated 25-mer oligonucleotide arms. Lane 1: negative control consisting of natural DNA (green) reacted with a Cy5-modified azide-terminated 25-mer oligonucleotide (red). Lane 2: three-arm stars are synthesized by grafting Cy5-modified azide-terminated 25-mer oligonucleotides to a 51-base-pair DBCO-dsDNA. Three-arm star polymers are indicated by overlap of Cy5 (red) and SYBR Gold (green) signals, thereby signifying a branched polymer product (yellow). (c) Analytical DHPLC chromatograms for purification of ssDNA symmetric homopolymeric three-arm stars monitored at 254 nm using the following method: linear gradient of 0%−100% acetonitrile/pH 7, 0.1 M TEAA buffer at a flow rate of 0.3 mL/min over 100 min using an Agilent reverse phase column. (d) Polyacrylamide gel electrophoresis of collected DHPLC peaks shows separation of template oligonucleotide from ssDNA symmetric three-arm star architecture (lanes 1−3). Empty lanes correspond to collected fractions with negligible signal at 254 nm.

Retardation of electrophoretic mobility for branched architectures is thought to be caused by a combination of increased molecular mass and topological entanglements within the confining gel pores.[43−46] Interestingly, three-arm star polymer products generally displayed complex banding patterns with two distinct bands on polyacrylamide gels. Nevertheless, MALDI mass spectrometry results clearly show that the linear backbone precursor contains only a single DBCO modification and that only a single branch is added following the grafting reaction (Table 1 and Figure S3). On the basis of this evidence, we believe that the dual banding pattern is likely due to the complexities of the electrophoretic mobility for nonlinear topologies in polyacrylamide gels rather than a cryptic branch

Table 1. Matrix-Assisted Laser Desorption/Ionization (MALDI) Mass Spectrometry Results for Branched Polymer Topologies Based on ssDNA Backbones

architecture	calculated m/z	determined m/z
three-arm star (25-mer DNA oligo arms)	24088.9	24133.5
AB_2 miktoarm star (one 10 kDa PEG branch)	27227.6	27015.6
AB_2 miktoarm star (one 1 kDa PEG branch)	17227.6	17279.2
symmetric H-polymer (17-mer DNA oligo branches)	28143.9	28433.1
asymmetric H-polymer (17-mer and 25-mer DNA oligo branches)	33011.1	33347.1
graft block copolymer (17-mer DNA oligo branches)	44539.9	44870.7
graft block copolymer (5-mer DNA oligo branches)	26287.8	26358.1

incorporation site. In particular, we conjecture that the dual banding could arise from one of two possibilities. First, it is possible that the single-stranded DNA backbone might be forming a cycle in the PAGE gel, which is run under native (nondenaturing) conditions. Although the linear ssDNA backbones are designed to minimize base pairing, it is possible that some amount of base pairing occurs in the linear backbone template in the gel. Second, we note that the native PAGE gel in Figure 2a was run before purification using DHPLC. Therefore, it is possible that for the 3-arm star one band corresponds to ssDNA backbone + branch and the second band corresponds to dsDNA backbone + branch. Nevertheless, following DHPLC and MALDI, we recover only a single product corresponding to the correct product molecular weight for a three-arm star polymer. In a second set of experiments, we synthesized three-arm star architectures using Cy5-modified azide-terminated 25-mer oligonucleotides, thereby allowing for direct visualization of the ssDNA branch in the three-arm star polymers within the polyacrylamide gel matrix (Figure 2b). Colocalization of Cy5 and SYBR Gold signals in the shifted gel band indicates formation of the three-arm star architecture (Figure 2b).

We next isolated the three-arm star polymer based on solely on ssDNA using DHPLC (Figure 2c). In order to purify three-arm star topologies from linear polymer precursors, we used a poly(styrene−divinylbenzene) column with 300 Å pore size. Fractions were collected based on peak intensity and subsequently concentrated and resuspended in ddH_2O for analysis via polyacrylamide gel electrophoresis (Figure 2d). In this way, DHPLC peaks can be correlated with electrophoretic mobility in order to determine separation resolution and product identity. Interestingly, the ssDNA three-arm star architecture shows a shorter retention time (25 min) compared to the complementary linear template oligonucleotide (27 min) under these conditions. We conjecture that this behavior could arise from a reduction in radius of gyration (R_g) for the branched polymer topology. Following DHPLC, we used MALDI mass spectrometry to determine the molecular weight of polymer samples in peak fractions (Table 1). In this way, we find that the three-arm star topology indeed corresponds to samples with reduced electrophoretic mobility (Figure S4), which also agrees with two-color fluorescence imaging in polyacrylamide gels.

The graft-onto synthesis method allows for the chemical identity of the side branches in a branched polymer to be varied in a fairly straightforward manner. To this end, we synthesized a

DOI: 10.1021/acs.macromol.5b00219
Macromolecules 2015, 48, 1296−1303

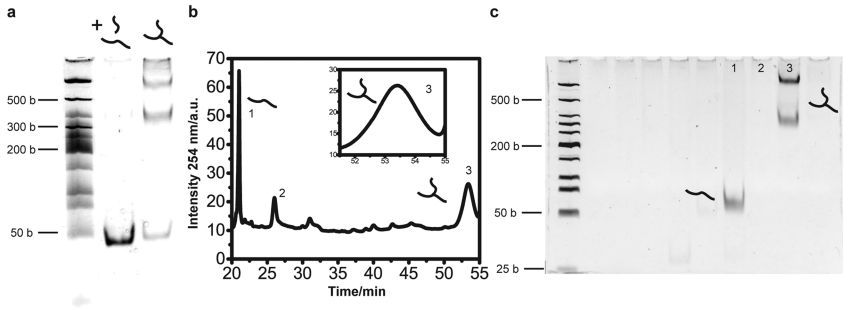

Figure 3. Synthesis of structurally defined AB_2 miktoarm star polymers. (a) Polyacrylamide gel electrophoresis of AB_2 miktoarm stars (A block: PEG, MW 10 kDa, B block: 25-mer oligonucleotide). Lane 1: negative control consisting of natural DNA backbones reacted with 10 kDa mPEG-azides. Lane 2: AB_2 miktoarm stars are synthesized by grafting azide-terminated mPEG to the central monomer of a 51-base-pair DNA. Formation of the branched polymer topology is indicated by the bands with reduced electrophoretic mobility and decrease of the DBCO-dsDNA linear backbone. (b) Analytical DHPLC trace for purification of the miktoarm star architecture was monitored at 254 nm using the following method: linear gradient of 0%−100% acetonitrile/pH 7, 0.1 M TEAA buffer at a flow rate of 0.3 mL/min over 100 min using an Agilent reverse phase column. (c) Polyacrylamide gel electrophoresis of collected DHPLC peaks shows separation of template oligonucleotide (lane 1) from miktoarm star architecture (lane 3). Multiple bands may be caused by polydispersity of the mPEG-azide as only the weight for the single branch product is found via MALDI. Empty lanes correspond to collected fractions with negligible signal at 254 nm.

AB_2 miktoarm star architecture consisting of one poly(ethylene glycol) (PEG) branch and two oligonucleotide branches. We began by linking a linear monofunctional mPEG-azide polymer (Creative PEGWorks, MW 10 kDa) to the central monomer (corresponding to base 26) of a 51-base-pair DBCO-dsDNA polymer. Polyacrylamide gel electrophoresis showed reduced mobility consistent with the formation of a branched polymer architecture as well as a multiple banding pattern observed for homopolymeric stars (Figure 3a). In this case, the multiple banding pattern could arise due to a combination of topology and the intrinsic polydispersity of the 10 kDa mPEG-azide polymer. Following synthesis, miktoarm stars are isolated using DHPLC on a poly(styrene−divinylbenzene) column with a 4000 Å pore size (Figure 3b). Polyacrylamide gel electrophoresis analysis of peak fractions obtained by DHPLC revealed nearly complete separation of the template oligonucleotide and miktoarm star architecture (Figure 3c), which was confirmed via MALDI mass spectrometry (Table 1 and Figure S5). In a second set of experiments, we decreased the average molecular weight of the PEG branch 10-fold (MW 1 kDa) and observed only a slight reduction in electrophoretic mobility compared to negative control reactions without DBCO-dsDNA. Nevertheless, the final miktoarm architecture was readily purified using DHPLC, followed by characterization using MALDI (Table 1 and Figures S6 and S7). Based on these results, this strategy allows for the synthesis of branched hybrid biopolymers with variable branch length and branch chemical identity.

Moving beyond homopolymer and heteropolymer three-arm stars, we also synthesized H-polymers, which consist of two branch points located at distal ends of a linear backbone (Figure 4). In this way, we effectively increased the structural complexity of the polymer topologies that are accessible using this method. First, a symmetric H-shape polymer was synthesized via attachment of azide-terminated oligonucleotide (17-mer dTTP) branches to monomers at positions 18 and 36 along a 53-base-pair dsDNA-DBCO template, thereby yielding an H-shaped polymer architecture with 17-mer branches and a 17-mer crossbar (Figure 4). Symmetric H-polymers showed a reduction in electrophoretic mobility similar to three-arm stars in the polyacrylamide gel matrix compared to negative control reactions in the absence of DBCO (Figure 4a). Interestingly,

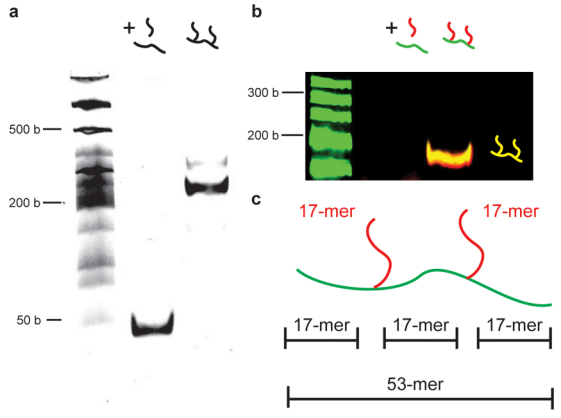

Figure 4. Synthesis of structurally defined H-polymers. (a) Polyacrylamide gel electrophoresis of symmetric H-polymers with 17-mer oligonucleotide arms. Lane 1: negative control consisting of natural DNA backbones reacted with an azide-terminated 17-mer oligonucleotide. Lane 2: synthesis of H-polymer by grafting azide-terminated 17-mer oligonucleotides to a 53-base-pair DBCO-dsDNA. Formation of the branched polymer topology is indicated by the bands with reduced electrophoretic mobility and absence of the DBCO-dsDNA linear backbone (b) Two-color fluorescence polyacrylamide gel electrophoresis of symmetric H-polymers containing Cy5-modified azide-terminated 17-mer oligonucleotide branches. Lane 1: negative control of natural DNA backbones reacted with a Cy5-modified azide-terminated 17-mer oligonucleotide. Lane 2: H-polymer architectures are indicated by overlap of Cy5 (red) and SYBR Gold (green) signals, thereby signifying a branched polymer product (yellow). (c) Schematic of symmetric H-polymer with 17-mer oligonucleotide branches and 17-mer oligonucleotide crossbar. Branches were attached at positions 18 and 36 along the 53-mer backbone.

the symmetric H-polymer architecture has a larger molecular weight (28.1 kDa) compared to the three-arm star architecture (24.1 kDa); however, the H-polymer sample generally exhibits a higher electrophoretic mobility in polyacrylamide gel. A higher mobility for H-polymers can be attributed to a combination of branch placement and branch number, such that terminally branched architectures behave more similarly to linear polymers, and addition of successive branches does not significantly change mobility, at least for low grafting

DOI: 10.1021/acs.macromol.5b00219
Macromolecules 2015, 48, 1296−1303

densities.[43−46] This effect may also contribute to the apparent weakening of the multiple banding pattern for H-polymers in polyacrylamide gels compared to 3-arm stars.

We also synthesized symmetric H-polymers using Cy5-modified azide-terminal 17-mer dTTP oligonucleotides. Two-color polyacrylamide gel electrophoresis clearly shows colocalization of Cy5 and SYBR Gold fluorescence signals, thereby indicating formation of symmetric H-polymer structures (Figure 4b). Symmetric H-polymers were also synthesized with homopolymeric dATP side branches, which behaved similarly to symmetric H-polymers with homopolymeric dTTP side branches (Figures S11−S14). Finally, we isolated the product H-polymer structures based on ssDNA using DHPLC, followed by molecular weight determination by MALDI (Table 1 and Figures S11−S14). In all cases, MALDI mass spectrometry confirmed the synthesis of the target H-polymer product.

We further increased the topological complexity of structurally defined polymers by synthesizing an asymmetric H-polymer architecture containing both a 17-mer and a 25-mer arm on each distal end of a crossbar. In particular, we attached azide-terminated 25-mer oligonucleotides to monomer positions 18 and 36 along a 53-base-pair dsDNA-DBCO product. Interestingly, the asymmetric H-polymer structure exhibited three shifted bands with the middle band visibly dominate in the polyacrylamide gel electrophoresis analysis (Figure 5a), which was not observed for the symmetric H-polymer architecture shown in Figure 4. Colocalization of Cy5 and SYBR Gold fluorescence signals in the polyacrylamide gel indicates the presence of branched architectures in all three bands (Figures 5b); however, this result alone does not rule out the possibility of a mixture of single- and double-branched architectures. In order to conclusively determine branch number and branch distribution among the reaction products, the asymmetric H-polymer sample was purified via DHPLC, followed by characterization and molecular weight determination by MALDI (Table 1 and Figures S15 and S16). Indeed, results from MALDI mass spectrometry revealed that H-polymer with two 25-mer oligonucleotide branches was synthesized as the major product, with no evidence of singly branched products from all collected DHPLC fractions.

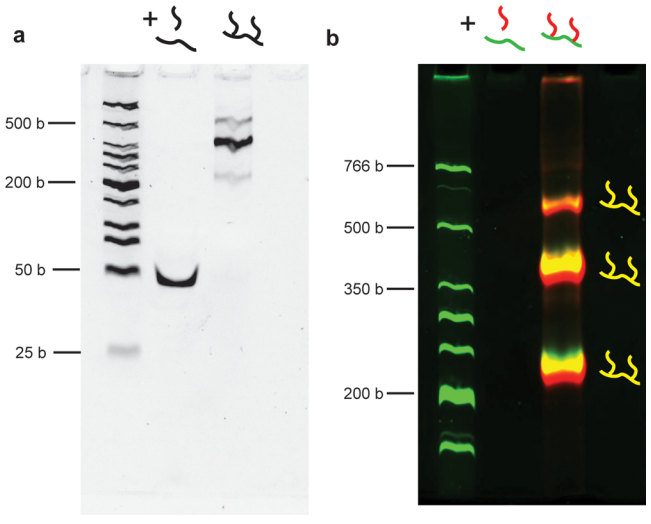

Figure 5. Synthesis of structurally defined asymmetric H-polymers. (a) Polyacrylamide gel electrophoresis of dsDNA H-polymer architecture with two 17-mer and two 25-mer oligonucleotide arms (dTTP). Lane 1: negative control consisting of natural DNA backbones reacted with an azide-terminated 25-mer oligonucleotide. Lane 2: synthesis of asymmetric H-polymer by grafting azide-terminated 25-mer oligonucleotides to a 53-base-pair DBCO-dsDNA. Formation of the branched polymer topology is indicated by the band with reduced electrophoretic mobility and absence of the DBCO-dsDNA linear backbone. (b) Two-color fluorescence polyacrylamide gel electrophoresis of asymmetric H-polymers containing Cy5-modified azide-terminated 25-mer oligonucleotide branches. Lane 1: negative control of natural DNA backbones reacted with a Cy5-modified azide-terminated 25-mer oligonucleotide. Lane 2: asymmetric H-polymer architectures are indicated by overlap of Cy5 (red) and SYBR Gold (green) signals, thereby signifying a branched polymer product (yellow).

Polymeric materials consisting of covalently attached immiscible blocks are of keen interest due to their self-assembly properties and emergent morphologies.[3] With a view toward increasing the topological complexity of DNA-based hybrid polymers, we next synthesized graft block copolymers, defined as macromolecules with multiple branches emanating from one end of a polymer backbone. Here, the grafted branches can be of identical or different chemical identity as the main-chain polymer backbone. We used the graft-onto synthesis method to design a graft block copolymer consisting of a main-chain oligonucleotide backbone with multiple oligonucleotide side branches (five branches each spaced five nucleotides apart). To this end, we attached azide-terminated 5-mer oligonucleotides at positions 1, 7, 13, 19, and 25 to a 50-base-pair DBCO-dsDNA product, which resulted in a reduction in electrophoretic mobility comparable to the three-arm star and H-polymer architectures (Figure S20). Similar to the asymmetric H-polymer sample, multiple bands were observed in the polyacrylamide gel electrophoresis analysis.

We further sought to conclusively determine branch number and branch distribution among the reaction products. In order to determine the identity of the branched polymer product(s), we used DHPLC to separate and isolate the graft block polymer architecture from the template oligonucleotide (Figure S20). MALDI mass spectrometry revealed that we obtained the full 5 branch graft block polymer architecture (Table 1 and Figure S21). Finally, we synthesized a graft block polymer with the same topology and branching architecture as the 5-mer branch product; however, it contained 17-mer oligonucleotide side branches (Figure 6). In this case, MALDI mass spectrometry revealed the presence of graft block polymer products containing 3 and 4 branches in the reaction mixture (Figures S22 and S23), which can be attributed to an increase in steric hindrance commonly observed with graft-onto synthesis methods.[3,15]

■ CONCLUSIONS

In this work, we demonstrate the synthesis of structurally defined three-arm stars, H-polymers, and graft block copolymers using a combination of template-directed PCR and copper-free "click" chemistry. Bioorthogonal DBCO branch sites are enzymatically incorporated by PCR in a template-dependent manner, followed by direct grafting of azide-terminated oligonucleotide branches to polymer backbones. Importantly, this method allows for precise placement of branches along the main-chain backbone, thereby resulting in monodisperse branched polymer products with tunable molecular weights and topologies. In all cases, branched polymer architectures are characterized by polyacrylamide gel electrophoresis, which generally shows retardation of electro-

DOI: 10.1021/acs.macromol.5b00219
Macromolecules 2015, 48, 1296−1303

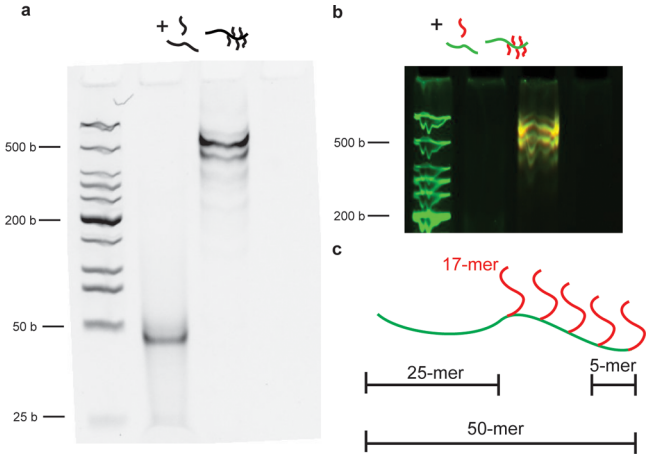

Figure 6. Synthesis of structurally defined graft block copolymers. (a) Polyacrylamide gel electrophoresis of dsDNA graft block copolymer architecture with five 17-mer oligonucleotide arms (dTTP). Lane 1: negative control consisting of natural DNA backbones reacted with an azide-terminated 17-mer oligonucleotide. Lane 2: synthesis of graft block copolymer by grafting azide-terminated 17-mer oligonucleotides to a 50-base-pair DBCO-dsDNA. Formation of the branched polymer topology is indicated by the band with reduced electrophoretic mobility and absence of the DBCO-dsDNA linear backbone. (b) Two-color fluorescence polyacrylamide gel electrophoresis of graft block copolymers containing Cy5-modified azide-terminated 17-mer oligonucleotide branches. Lane 1: negative control of natural DNA backbones reacted with a Cy5-modified azide-terminated 17-mer oligonucleotide. Lane 2: graft block copolymer architectures are indicated by overlap of Cy5 (red) and SYBR Gold (green) signals, thereby signifying a branched polymer product (yellow). (c) Schematic of graft block copolymer with 17-mer oligonucleotide branches spaced 5-mer apart. Branches were attached at positions 1, 7, 13, 19, and 25 along the 50-mer backbone.

phoretic mobility as a function of branch length, branch number, and branch placement. We further purify and isolate the desired branched polymer structures from their linear template precursors via DHPLC, followed by molecular weights determination by MALDI.

Moving beyond oligonucleotide branches, the method developed in this work provides a versatile platform to synthesize structurally defined branched heteropolymers. To this end, we synthesized AB_2 miktoarm star architectures with PEG-azide branches of tunable size. These hybrid architectures show similar shifts in electrophoretic mobility based on branch length as the homopolymeric three-arm star counterparts. In fact, this work has recently motivated a related study in our group on the synthesis and direct visualization of single-branched polymers using single molecule fluorescence microscopy. Overall, this synthetic platform allows for design of branched architectures with compositional and topological uniformity.

In future work, this synthetic method can be used to systematically study structure–function relationships by controlling branch placement, branch number, and chemical identity of side branches. In this way, we believe that controlled polymer topologies can be used to drive assembly of new materials for biomedical and electronic materials applications.[3] Finally, this platform offers the ability to study the effects of architectural defects on microstructural assembly.[3] To this end, the unique ability to insert site-specific errors (e.g., missing branches or distinct chemical functionalities) holds the potential to enable systematic characterization of macromolecular behavior for advanced materials.

■ ASSOCIATED CONTENT

Supporting Information

DNA sequences, polyacrylamide gel electrophoresis, DHPLC, and MALDI mass spectrometry analysis for three-arm stars, miktoarm stars, H-polymers, and graft block copolymers. This material is available free of charge via the Internet at http://pubs.acs.org.

■ AUTHOR INFORMATION

Corresponding Author

*E-mail: cms@illinois.edu (C.M.S.).

Notes

The authors declare no competing financial interest.

■ ACKNOWLEDGMENTS

We acknowledge facilities at the Roy J. Carver Biotechnology Center, the Metabolomics Research Center, and the School of Chemical Sciences Mass Spectrometry Laboratory at the University of Illinois at Urbana–Champaign. The authors thank Elijah Karvelis for his contributions to experiments. This research was supported by a Packard Fellowship from the David and Lucille Packard Foundation, an NSF CAREER Award (CBET 1254340), and the Camille and Henry Dreyfus Foundation.

■ REFERENCES

(1) Lutz, J.-F.; Ouchi, M.; Liu, D. R.; Sawamoto, M. *Science* **2013**, *341*, 1238149-1–1238149-8.
(2) Matyjaszewski, K. *Science* **2011**, *333*, 1104–1105.
(3) Matyjaszewski, K.; Tsarevsky, N. V. *Nat. Chem.* **2009**, *1*, 276–288.
(4) Matyjaszewski, K. *Prog. Polym. Sci.* **2005**, *30*, 858–875.
(5) Whitesides, G. M.; Grzybowski, B. *Science* **2002**, *295*, 2418–2421.
(6) Marciel, A. B.; Schroeder, C. M. *J. Polym. Sci., Part B: Polym. Phys.* **2013**, *51*, 556–566.
(7) Hill, D. J.; Mio, M. J.; Prince, R. B.; Hughes, T. S.; Moore, J. S. *Chem. Rev.* **2001**, *101*, 3893–4012.
(8) Hawker, C. J.; Wooley, K. L. *Science* **2005**, *309*, 1200–1205.
(9) Braunecker, W. A.; Matyjaszewski, K. *Prog. Polym. Sci.* **2007**, *32*, 93–146.
(10) Bai, L.; Zhang, L.; Cheng, Z.; Zhu, X. *Polym. Chem.* **2012**, *3*, 2685–2697.
(11) Hadjichristidis, N.; Iatrou, N.; Pitsikalis, M.; Mays, J. *Prog. Polym. Sci.* . **2006**, *31*, 1068–1132.
(12) Matyjaszewski, K. *Polym. Int.* **2003**, *52*, 1559–1565.
(13) Whittaker, M. R.; Urbani, C. N.; Monteiro, M. J. *J. Am. Chem. Soc.* **2006**, *128*, 11360–11361.
(14) Gao, H.; Matyjaszewski, K. *Macromolecules* **2006**, *29*, 4960–4965.
(15) Gao, H.; Matyjaszewski, K. *J. Am. Chem. Soc.* **2007**, *129*, 6633–6639.
(16) Tsarevsky, N. V.; Bencherif, S. A.; Matyjaszewski, K. *Macromolecules* **2007**, *40*, 4439–4445.
(17) Neugebauer, D.; Zhang, Y.; Pakula, T.; Sheiko, S. S.; Matyjaszewski, K. *Macromolecules* **2003**, *36*, 6746–6755.
(18) Johnson, J. A.; Lewis, D. R.; Diaz, D. D.; Finn, M. G.; Koberstein, J. T.; Turro, N. J. *J. Am. Chem. Soc.* **2006**, *128*, 6564–6565.
(19) Pinheiro, A. V.; Han, D.; Shih, W. M.; Yan, H. *Nat. Nanotechnol.* **2011**, *6*, 763–772.
(20) Keller, S.; Marx, A. *Chem. Soc. Rev.* **2011**, *40*, 5690–5697.
(21) Roh, Y. H.; Ruiz, R. C. H.; Peng, S.; Lee, J. B.; Luo, D. *Chem. Soc. Rev.* **2011**, *40*, 5730–5744.

DOI: 10.1021/acs.macromol.5b00219
Macromolecules 2015, 48, 1296–1303

(22) Paredes, E.; Zhang, X.; Ghodke, H.; Yadavalli, V. K.; Das, S. R. *ACS Nano* **2013**, *7*, 3953−3961.
(23) Kwak, M.; Herrmann, A. *Angew. Chem., Int. Ed.* **2010**, *49*, 8574−8587.
(24) Ding, K.; Alemdaroglu, F. E.; Borsch, M.; Berger, R.; Herrmann, A. *Angew. Chem., Int. Ed.* **2007**, *46*, 1172−1175.
(25) Li, Z.; Zhang, Y.; Fullhart, P.; Mirkin, C. A. *Nano Lett.* **2004**, *4*, 1055−1057.
(26) Cottenye, N.; Syga, M.-I.; Nosov, S.; Muller, A. H. E.; Ploux, L.; Vebert-Nardin, C. *Chem. Commun.* **2012**, *48*, 2615−2617.
(27) Taira, S.; Yokoyama, K. *Biotechnol. Bioeng.* **2004**, *88*, 35−41.
(28) Watson, K. J.; Park, S.-J.; Im, J.-H.; Nguyen, S. T.; Mirkin, C. A. *J. Am. Chem. Soc.* **2001**, *123*, 5592−5593.
(29) Gibbs, J. M.; Park, S.-J.; Anderson, D. R.; Watson, K. J.; Mirkin, C. A.; Nguyen, S. T. *J. Am. Chem. Soc.* **2005**, *127*, 1170−1178.
(30) Chen, P.; Li, C.; Liu, D.; Li, Z. *Macromolecules* **2012**, *45*, 9579−9584.
(31) James, C. R.; Rush, A. M.; Insley, T.; Vukovic, L.; Adamiak, L.; Kral, P.; Gianneschi, N. C. *J. Am. Chem. Soc.* **2014**, *136*, 11216−11219.
(32) Umeno, D.; Kawasaki, M.; Maeda, M. *Bioconjugate Chem.* **1998**, *9*, 719−724.
(33) Maeda, M.; Nishimura, C.; Umeno, D.; Takagi, M. *Bioconjugate Chem.* **1994**, *5*, 527−531.
(34) Umeno, D.; Maeda, M. *Anal. Sci.* **1997**, *13*, 553−556.
(35) Baccaro, A.; Marx, A. *Chem.—Eur. J.* **2010**, *16*, 218−226.
(36) Kuwahara, M.; Takahata, Y.; Shoji, A.; Ozaki, H.; Sawai, H. *Bioorg. Med. Chem. Lett.* **2003**, *13*, 3735−3738.
(37) Kasahara, Y.; Kuwahara, M. *J. Nucleic Acids* **2012**, *2012*, 1−13.
(38) Xiao, W.; Oefner, P. J. *Hum. Mutat.* **2001**, *17*, 439−474.
(39) Agard, N. J.; Prescher, J. A.; Bertozzi, C. R. *J. Am. Chem. Soc.* **2004**, *126*, 15046−15047.
(40) Gutsmiedl, K.; Fazio, D.; Carell, T. *Chem.—Eur. J.* **2010**, *16*, 6877−6883.
(41) Baskin, J. M.; Prescher, J. A.; Laughlin, S. T.; Agard, N. J.; Chang, P. V.; Miller, I. A.; Lo, A.; Codelli, J. A.; Bertozzi, C. R. *Proc. Natl. Acad. Sci. U. S. A.* **2007**, *104*, 16793−16797.
(42) Khanna, K.; Varshney, S.; Kakkar, A. *Polym. Chem.* **2010**, *1*, 1171−1185.
(43) Heuer, D. M.; Saha, S.; Kusumo, A. T.; Archer, L. A. *Electrophoresis* **2004**, *25*, 1772−1783.
(44) Heuer, D. M.; Yuan, C.; Saha, S.; Archer, L. A. *Electrophoresis* **2005**, *26*, 64−70.
(45) Heuer, D. M.; Saha, S.; Archer, L. A. *Biopolymers* **2003**, *70*, 471−481.
(46) Lau, H. W.; Archer, L. A. *Phys. Rev. E* **2011**, *84*, 061916-1−061916-7.

DOI: 10.1021/acs.macromol.5b00219
Macromolecules 2015, 48, 1296−1303